Received: 7 February 2022 | Revised: 1 August 2022 | Accepted: 5 August 2022

DOI: 10.1002/jmor.21504

RESEARCH ARTICLE

JOURNAL OF morphology WILEY

Porosomes in uterine epithelial cells: Ultrastructural identification and characterization during early pregnancy

Sadaf N. Kalam | Samson Dowland | Laura Lindsay | Christopher R. Murphy

School of Medical Sciences, Faculty of Medicine and Health, The University of Sydney, Sydney, New South Wales, Australia

Correspondence
Sadaf N. Kalam, Faculty of Medicine and Health, Room G54, Medical Foundation Bldg (K25), The University of Sydney, Sydney, NSW 2006, Australia.
Email: skal5494@uni.sydney.edu.au and sadaf199@hotmail.com

Abstract

Porosomes are plasma membrane structures in secretory cells that allow transient docking and/or partial fusion of vesicles during which they release their content then disengage. This is referred to as "kiss and run" exocytosis. During early pregnancy, at the time of receptivity, there is a high level of vesicle activity in uterine epithelial cells (UECs). One of the secretory pathways for these vesicles could be via porosomes, which have yet to be identified in UECs. This study identified porosomes in the apical plasma membrane of UECs for the first time. These structures were present on days 1, 5.5, and 6 of early pregnancy, where they likely facilitate partial secretion via "kiss and run" exocytosis. The porosomes were measured and quantified on days 1, 5.5, and 6, which showed there are significantly more porosomes on day 5.5 (receptive) compared to day 1 (nonreceptive) of pregnancy. This increase in porosome numbers may reflect major morphological and molecular changes in the apical plasma membrane at this time such as increased cholesterol and soluble NSF attachment protein receptor proteins, as these are structural and functional components of the porosome complex assembly. Porosomes were observed in both resting (inactive) and dilated (active) states on days 1, 5.5, and 6 of early pregnancy. Porosomes on day 5.5 are significantly more active than on day 1 as demonstrated by the dilation of their base diameter. Further two-way ANOVA analysis of base diameter in resting and dilated states found a significant increase in porosome activity in day 5.5 compared to day 1. This study therefore indicates an increase in the number and activity of porosomes at the time of uterine receptivity in the rat, revealing a mechanism by which the UECs modify the uterine luminal environment at this time.

KEYWORDS

exocytosis, implantation, kiss and run, polarised membrane traffic, uterine receptivity, vesicles

LinkedIn: www.linkedin.com/in/sadaf-kalam-b6272085

1 | INTRODUCTION

Secretions from the uterine epithelium play an important role in providing a specialized environment for fertilization, embryo development, and implantation (Gandolfi, 1995; Nieder & Macon, 1987). Uterine secretions come from a combination of fluid transport from ion and water channels and the release of vesicular content via exocytosis (Kalam et al., 2020; Lindsay & Murphy, 2006; McManaman et al., 2006). High levels of vesicular activity are seen in uterine epithelial cells (UECs) during uterine receptivity (Kalam et al., 2020; Murphy, 2004; Parr, 1982) and it is likely that the exocytosis from UECs, contribute to the changes in uterine fluid volume and content, which influences embryo implantation and development (De Los Santos et al., 2016; O'Neil et al., 2020; Strandell & Lindhard, 2002).

In all eukaryotic cells, secretions are produced by exocytosis of vesicles (Alberts et al., 2008). There are many methods of exocytosis that cells can utilize. The most common method is full fusion exocytosis, which involves transport of vesicles from the Golgi apparatus to target plasma membranes where membranes of the vesicles fuse, releasing vesicular content outside the cell (Burgess & Kelly, 1987; Jamieson & Palade 1967a, 1967b; Schramm, 1967). Secretion can also take place via other exocytotic routes such as compound exocytosis, lysosomal secretion, extracellular vesicle secretion, and "kiss and run" exocytosis (Antonyak & Cerione, 2014; Battey et al., 1999; Harata et al., 2006; Holt et al., 2006; Pickett & Edwardson, 2006; Taguchi, 2013; Tkach & Thé Ry, 2016; Tuma & Hubbard, 2003).

In "kiss and run" exocytosis (Figure 1) vesicles expel a portion of their content without full fusion of the vesicular membrane with the plasma membrane (Ceccarelli et al., 1972). Vesicles can accomplish this fractional secretion with the involvement of a plasma membrane ultrastructure called a "porosome". Porosomes (Figure 2) allow the transient docking and/or partial fusion of vesicles, during which they release their content then disengage (Naik et al., 2015). Porosomes are cup-shaped supramolecular lipoprotein structures located in the apical plasma membrane of secreting cells. Their diameters range from 15 nm in neurons and astrocytes to 100–180 nm in endocrine and exocrine cells (Aravanis et al., 2003; Lee et al., 2009; Taraska et al., 2002). All exocytotic events, including "kiss and run" via porosomes, are regulated by a family of SNAP receptors (SNARE) (soluble NSF attachment proteins [SNAPs]) proteins. SNARE proteins traffic vesicles by pairing a vesicle SNARE (v-SNARE) with a target SNARE (t-SNARE) that pulls the membranes together (Söllner et al., 1993; Sutton et al., 1998).

During uterine receptivity, the UECs undergo many molecular and morphological changes including loss of microvilli, reorganization of the apical terminal web and an increase in apical lipid rafts and adhesion proteins. These changes are collectively referred to as plasma membrane transformation (Murphy, 1994, 2004). These changes are likely to be mediated by the increase in the number of apical vesicles on day 5, the beginning of uterine receptivity in the rat

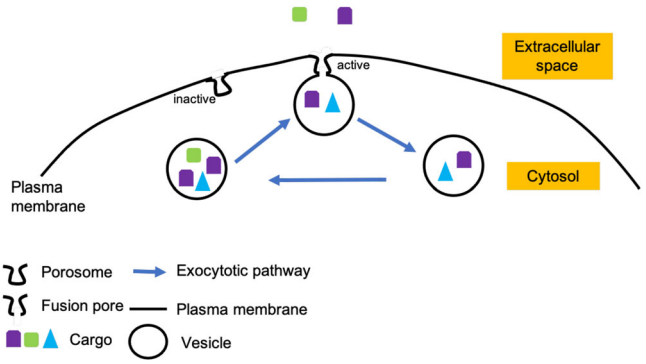

FIGURE 1 "Kiss and run" exocytosis. In "Kiss and Run" exocytosis, a vesicle docks onto a porosome on the plasma membrane and releases its cargo into the extracellular space without the vesicular membrane fusing onto the plasma membrane. Porosomes without vesicles docked are inactive and docked are active. This vesicle then disengages from the porosome and can be replenished for further "kiss and run" exocytosis.

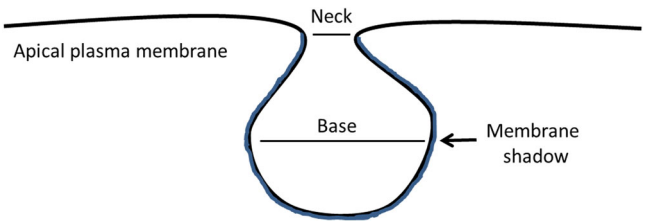

FIGURE 2 Schematic diagram showing the structural characteristics of a porosome. Porosomes are cup-shaped supramolecular lipoprotein structures located in the apical plasma membrane of secreting cells, with a narrow opening neck and a wide base.

(Parr, 1982). On day 5.5 of pregnancy, exocytosis is observed in UECs with an increase in exocytotic SNARE protein (VAMP2 and syntaxin 3) signaling in the apical region of UECs (Kalam et al., 2020). However, the complete plasma membrane fusion of all apical vesicles seen on day 5 would result in a significant increase in the surface area of the plasma membrane by day 6, but this is not observed (Poste & Allison, 1973; Preston et al., 2006). Instead there is a decrease in plasma membrane area seen by the loss of microvilli on day 6 (Enders & Schlafke, 1967; Murphy, 1993; Preston et al., 2006; Tachi et al., 1970). This implies full fusion exocytosis is not the only method of secretion that UECs employ to secrete vesicular content to the apical surface during uterine receptivity.

Porosomes have yet to be identified or characterized during early pregnancy in UECs, but during uterine receptivity in early pregnancy there is high vesicular activity in the apical area of UECs (Murphy & Martin, 1987; Parr, 1982). These vesicles may thus be using the "kiss and run" exocytosis model via porosomes to contribute to uterine secretions. The present investigation thus hypothesized that porosomes are located in the apical plasma membrane of UECs during uterine receptivity.

2 | MATERIALS AND METHODS

2.1 | Animals and mating

This study used virgin female Wistar rats aged 10–12 weeks. All procedures were approved by the University of Sydney Animal Ethics Committee. Rats were housed in plastic cages at 21°C under a 12 h light–dark cycle and were provided with free access to food and water. Prooestrus female rats were mated overnight with males of proven fertility. The presence of sperm in a vaginal smear the following morning indicated successful mating, and this was designated day 1 of pregnancy. Uterine tissue was collected from four rats each from days 1, 5.5, and 6 of pregnancy. In total, 12 rats were used for this study.

2.2 | Tissue collection

Rats were administered 20 mg/kg of sodium pentobarbitone (Vibac Animal Health) intraperitoneally and the uterine horns were collected under deep anesthesia before euthanasia. Uterine horns were removed and processed for transmission electron microscopy.

2.3 | Transmission electron microscopy (TEM)

Uteri were cut into 5 mm pieces and were directly fixed in Karnovsky's fixative (2.5% glutaraldehyde [ProSciTech], 2% paraformaldehyde [ProSciTech] in 0.1mol l^{-1} Sorenson's phosphate buffer [PB, pH 7.4]) for 45 min at room temperature. The tissue was then further cut into 0.5–1 mm slices under a droplet of fixative and returned to fresh fixative for another 45 min. The tissue was washed in 0.1 mol l^{-1} PB then postfixed for an hour with 1% osmium tetroxide (OsO_4) in 0.1 mol l^{-1} PB, containing 0.8% potassium ferricyanide to enhance the contrast of the plasma membrane (Karnovsky, 1971). Tissue was rinsed in 0.1 mol l^{-1} PB and incubated in 2% OsO_4 solution (in 0.1 mol l^{-1} PB) for 10 min to remove any unreacted potassium ferricyanide (Hoshino et al., 1976). Tissue was washed with MilliQ water and dehydrated with graded series of ethanol, then infiltrated with Spurr's resin (SPI supplies). Uterine slices were embedded in fresh Spurr's resin in BEEM® capsules (ProSciTech) and polymerized at 60°C for 24 h. Two blocks per animal were cut at 60–70 nm using a Leica Ultracut S ultramicrotome (Leica) and mounted onto 400-mesh copper grids. Sections were poststained with a saturated solution of uranyl acetate in 50% ethanol for 45 min and then by Reynold's lead citrate for 10 min. Sections were examined in a Jeol 1011 TEM (Jeol Ltd.) at 80kV and imaged with a Gatan SC200 Orius CCD Camera (Gatan Inc.).

2.4 | Identifying and characterizing porosomes in UECs

Porosomes were identified as a flask-shaped membrane depression/invagination with an apical neck, a rounded base, and an electron dense shadow referred to as an anchoring cable/tether (Figure 2; Craciun & Barbu-Tudoran, 2013). These porosomes are found as part of the apical plasma membrane of the luminal UECs. To be classified as a porosome the base diameter had to be wider than the neck, with a maximum base diameter of 150 nm. These porosomes were further classified as resting or dilated, demonstrating their secretory activity status (Jena, 2004, 2009; Schneider et al., 1997). Porosomes with a base diameter below 50 nm were classified as resting porosomes, while those with a base diameter above 50 nm were classified as dilated.

2.5 | Counting and measuring porosomes

25 images were taken at ×50,000 magnification per grid. Two grids per block were obtained from two different blocks per animal. Thus, a total of 100 images were taken per animal for these porosome measurements. Porosomes were identified, measured, and quantified with Image J software (Image J; National Institutes of Health). The apical plasma membrane of UECs from days 1, 5.5, and 6 of pregnancy was measured by tracing the membrane surface (including all projections and invaginations) and the numbers of porosomes were counted along this region. The number of porosomes is reported as number of porosomes/μm plasma membrane.

The base diameter of porosomes was also measured since it provides information about the level of secretory activity of porosomes on days 1, 5.5, and 6 of pregnancy and statistical analysis was performed.

2.6 | Statistical analysis

Statistical analysis was performed to determine differences in porosome count and activity between days 1, 5.5, and 6 with GraphPad Prism Software (Version 7; GraphPad Software, Inc.). The difference in the number of porosomes on days 1, 5.5, and 6 was analyzed with one-way analysis of variance (ANOVA). For multiple comparisons, Tukey's post hoc test was applied (reporting multiplicity-adjusted p-values) to determine which pairs of means were significantly different. The change in porosome activity on days 1, 5.5, and 6 was analyzed with a two-way ANOVA. For multiple comparisons, Tukey's post hoc test was applied (reporting multiplicity-adjusted p-values) to determine which pairs of means were significantly different. Probability values of $p < .05$ were considered significant. All graphs were generated using GraphPad Prism Software and demonstrate the mean ± standard error of the mean.

3 | RESULTS

3.1 | Porosomes are present in the apical plasma membrane of UECs

Porosomes were observed to be present as part of the apical plasma membrane of UECs on days 1, 5.5, and 6 of pregnancy (Figure 3).

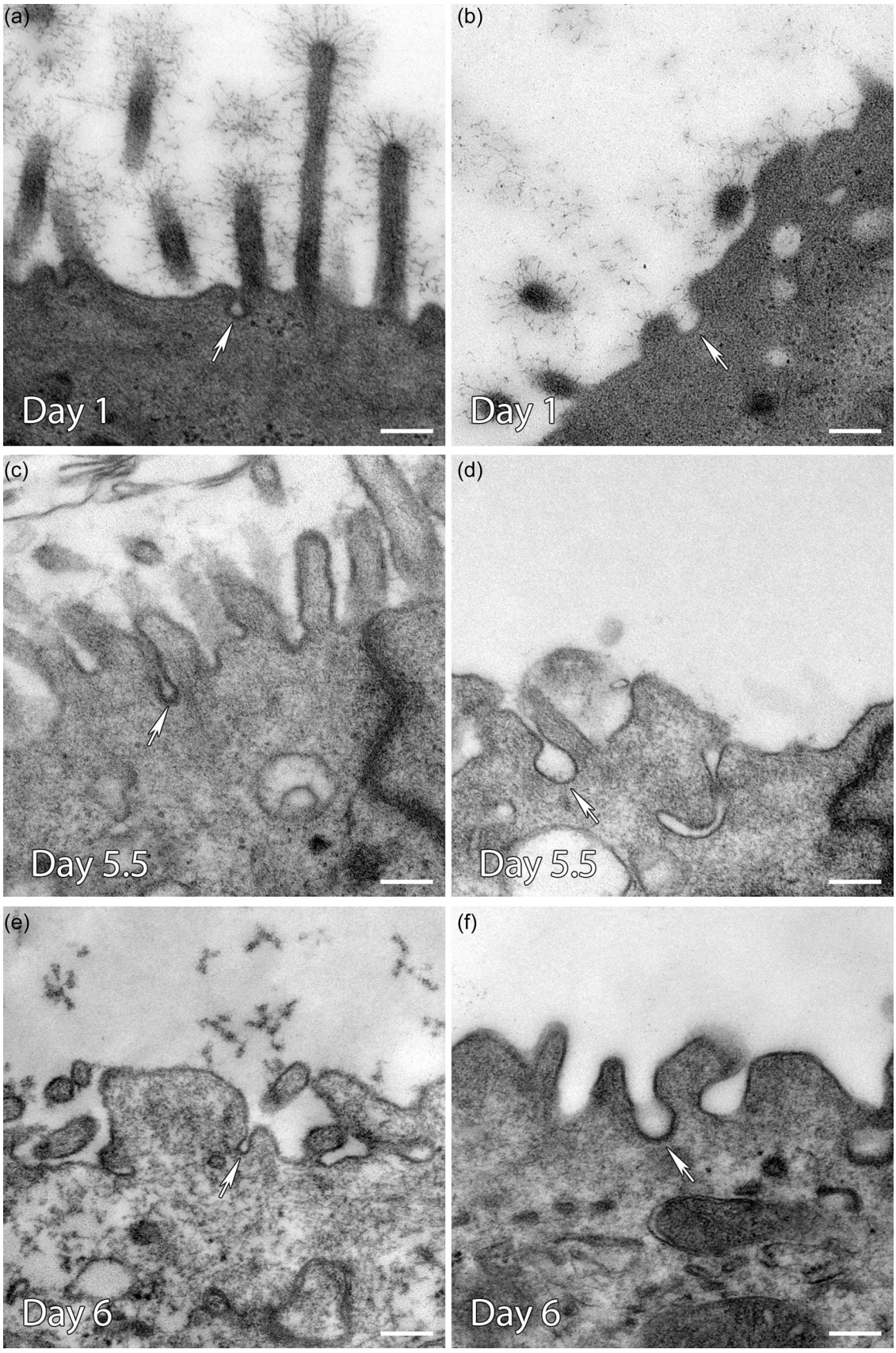

FIGURE 3 Transmission electron microscopy of the apical plasma membrane of uterine epithelial cells from days 1, 5.5, and 6 of early pregnancy. On day 1 of pregnancy, prosomes (arrow) are found in a resting state (a) or a dilated state (b). On day 5.5 of pregnancy prosomes (arrow) are seen in their resting state (c) or their dilated state (d). On day 5.5 of pregnancy prosomes (arrow) are observed in their resting state (e) or their dilated state (f). All scale bars are 200 nm.

These porosomes were seen in resting and dilated states, indicating differences in secretory activity on day 1 (Figure 3a,b), day 5.5 (Figure 3c,d), and day 6 (Figure 3e,f) of pregnancy (analysis below). Traced porosomes (rest vs. active) are highlighted in Figure 4 showing the neck and base regions.

3.2 | Total porosome numbers increase on day 5.5 of pregnancy

Porosomes were counted on each day of pregnancy and standardized to 1 μm unit plasma membrane (Figure 5). On day 1 of the pregnancy, there were 0.066 porosomes per 1 μm plasma membrane. On day 5.5 of pregnancy, the number of porosomes significantly increased to 0.174 porosomes per 1 μm plasma membrane compared to day 1 (one-way ANOVA, $n = 4$, $p = .0369$). On day 6 of pregnancy, porosome numbers were 0.130 porosomes per 1 μm plasma membrane, which was not significantly different to other days.

3.3 | Porosome activity during early pregnancy

The activity status of each porosome was determined based on their base diameter and the number of active vs inactive porosomes was compared on each day of pregnancy (Figure 6). On day 1 of pregnancy (Figure 6), 69% of porosomes were seen to be dilated (base diameter 51.0–115.6 nm) and the remaining 31% in a resting state (base diameter 28.3–50.0 nm). On day 5.5 of pregnancy, 71% of porosomes are dilated (base diameter 51.0–150.0 nm) with the remaining 29% in a resting configuration (base diameter 15.7–50.0 nm). On day 6, 63% are dilated (base diameter 51.0–150.0 nm) and 37% are in a resting state (base diameter 15.9– 50 nm; Figure 6). These ranges were averaged each day and presented in Table 1.

In the dilated state, there was a significant increase in the base diameter on day 5.5 compared to day 1 (two-way ANOVA, $n = 4$, $p = .0003$) and on day 6 compared to day 1 (two-way ANOVA, $n = 4$, $p = .0104$) (Figure 7).

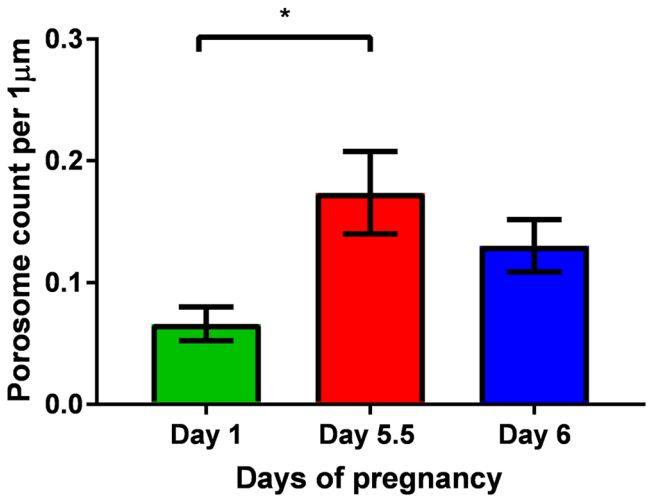

FIGURE 5 Porosome count per 1 μm of apical plasma membrane of uterine epithelial cells on days 1, 5.5, and 6 during early pregnancy. Statistical analysis (one-way analysis of variance) found a significant increase in the number of porosomes per μm of apical plasma membrane on day 5.5 compared to 1 of early pregnancy. Bars represent the mean ± standard error of the mean, $n = 4$; (*$p < .05$).

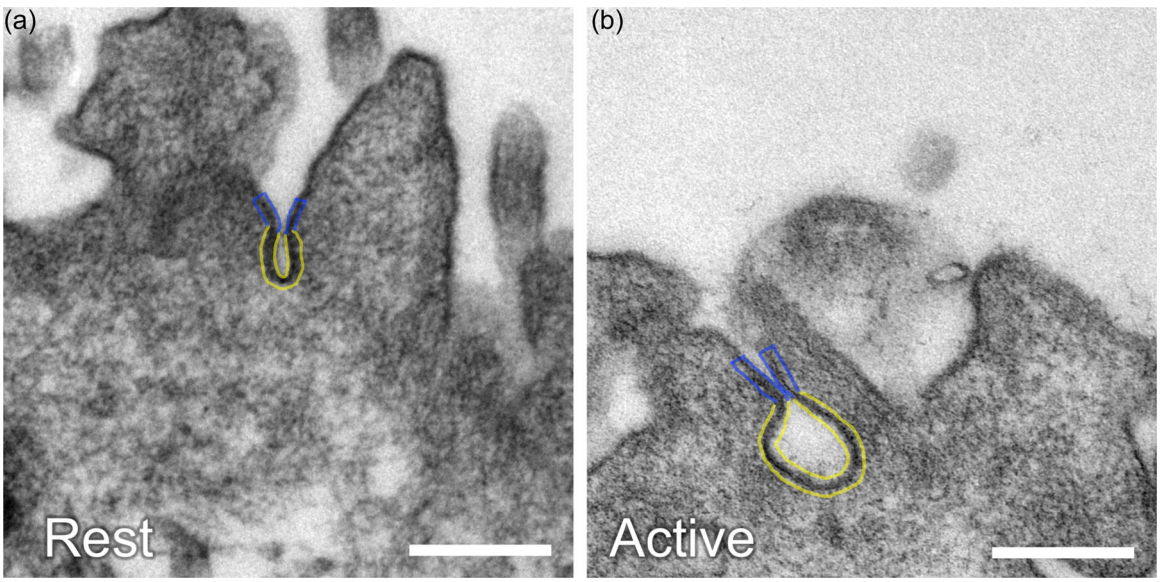

FIGURE 4 Transmission electron microscopy of the apical plasma membrane of uterine epithelial cells with traced porosomes at rest and active state. Porosomes at a resting state traced with yellow to highlight the base and blue to highlight the neck on day 6 of pregnancy in uterine epithelial cells (a). Active porosome with yellow highlighted base and neck highlighted blue as seen on day 5.5 of pregnancy (b). All scale bars are 200 nm.

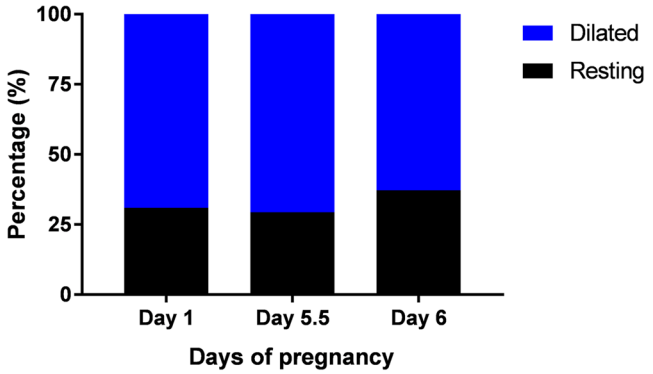

FIGURE 6 Percentage of porosome activity in uterine epithelial cells during early pregnancy. Stacked graph showing the percentage of resting versus dilated porosomes in days 1, 5.5, and 6 of early pregnancy; $n = 4$. On day 1 of pregnancy, 69% of porosomes were seen to be dilated and the remaining 31% are resting. On day 5.5, 71% of porosomes are dilated with the remaining 29% resting. On day 6, 63% are dilated and 37% are resting.

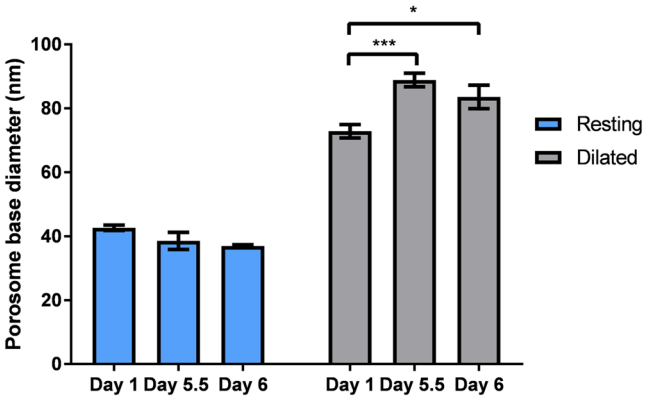

FIGURE 7 Comparison of the average base diameters of porosomes in the resting and dilated states in days 1, 5.5, and 6 of early pregnancy. Statistical analysis (two-way analysis of variance [ANOVA]) showed no significant difference in base diameter in the resting state on days 1, 5.5, and 6. Two-way ANOVA found a significant increase in the base diameter of porosomes on day 5.5 compared to 1 of early pregnancy; and on day 6 compared to day 1 in the dilated state. Bars represent the mean ± standard error of the mean, $n = 4$; ($^{*}p < .05$; $^{***}p < .001$).

TABLE 1 Average neck and base porosome diameter at resting and dilated state in uterine epithelial cells on days 1, 5.5, and 6

	Average porosome diameter (nm)			
	Resting		Dilated	
Days	Neck	Base	Neck	Base
1	24.355	42.653	35.514	72.813
5.5	18.425	38.568	33.140	88.841
6	13.632	36.969	24.394	83.585

4 | DISCUSSION

This is the first study to identify porosomes in the apical plasma membrane of UECs. Porosomes were present in both resting (inactive) and dilated (active) states on days 1, 5.5, and 6 of early pregnancy. Porosomes are part of the secretory machinery in cells and have previously been seen in chromaffin cells of the adrenal medulla (S. J. Cho, Wakade, et al., 2002), growth hormone secreting cells of the pituitary gland (S. J. Cho, Wakade, et al., 2002), neurons (W. J. Cho et al., 2004; Tojima et al., 2000), astrocytes (W. J. Cho, Ren, et al., 2009; Lee et al., 2009), β-cells of the endocrine pancreas, mast cells (Jena, 2004), hair cells (Drescher et al., 2011) and respiratory epithelium (Hou et al., 2014). Thus, the presence of porosomes in UECs shows that partial secretion also known as "kiss and run" secretion (Ceccarelli et al., 1972) is taking place throughout early pregnancy in both nonreceptive and receptive UECs.

Our study further measured and counted these porosomes on days 1, 5.5, and 6 of pregnancy and found a significant increase in the number of porosomes on day 5.5 compared to day 1 of pregnancy. This increase in porosome count on day 5.5 (uterus receptive for blastocyst implantation) compared to day 1 (nonreceptive uterus) may play a role in the dramatic morphological and molecular changes that occur in the apical plasma membrane at this time (Murphy, 1994, 2001, 2004). There is an increase in cholesterol content and SNARE proteins (v-SNARE: VAMP2 and t-SNAREs: syntaxin 3) apically in UECs during uterine receptivity (Kalam et al., 2020; Murphy & Dwarte, 1987; Murphy & Martin, 1985). Both plasma membrane cholesterol and SNARE proteins are known to participate in the integrity and structure of the porosome complex (W. J. Cho et al., 2007; Jeremic et al., 2006, 2003).

Not only is there an increase in porosome number at the time of receptivity, there is also an increase in porosome activity at this time. The study found porosomes were participating in secretion, seen by the dilation of the porosome base. The increase in porosome base diameter, which was from resting to dilated, was within the range (25%–45%) observed in other cells like pancreatic acinar cells, which is a secretory epithelial cell (Schneider et al., 1997).

The porosome ring complex found in the base of the porosome (Jeremic et al., 2003; Schneider et al., 1997), is considered to be composed of cholesterol (Jeremic et al., 2006) and several different proteins including calcium channels, t-SNAREs: SNAP23/25 and syntaxin 1 (W. J. Cho et al., 2005, 2004). Cholesterol is required as a major component of the porosome complex for its structural integrity and function (W. J. Cho et al., 2007; Jeremic et al., 2006). Atomic force microscopy (AFM) studies have previously shown that depletion of cholesterol in neurons resulted in dissociation of SNAP25, syntaxin 1 and calcium channels from the neural porosome (Jeremic et al., 2006). In regulated exocytosis, SNARE-induced membrane fusion requires calcium (S. J. Cho, Wakade, et al., 2002; Jeremic, Cho, et al., 2004; Jeremic, Kelly, et al., 2004) and the loss of interaction between SNAP25, syntaxin 1, and calcium channels at the neural porosome complex affects the assembly and stability of the neural porosome (W. J. Cho et al., 2007).

During uterine receptivity there is an increase in cholesterol in the apical plasma membrane of UECs (Murphy & Dwarte, 1987). This rise in plasma membrane cholesterol could be contributing to the assembly of porosomes on the UEC surface, resulting in the significant expansion in porosome numbers that is observed in this study. Plasma membrane cholesterol is known as a vesicle fusion docking site assisting with cell secretion, since cholesterol areas are more energy favorable for vesicles to dock (Epand, 2006). The increase in plasma membrane cholesterol in UEC surface during uterine receptivity (Murphy & Martin, 1987) could be aiding full fusion exocytosis that results in complete membrane fusion and secretion but also partial secretions via porosomes.

SNARE proteins along with cholesterol are integral parts of the porosome ring complex found in the base of the porosome (W. J. Cho, Shin, et al., 2009; Mohrmann et al., 2010). SNARE proteins are involved in directing secretory vesicles to dock and fuse with the plasma membrane-associated porosomes and to release their contents (S. J. Cho, Wakade, et al., 2002; Jeremic, Cho, et al., 2004; Jeremic, Kelly, et al., 2004). Studies using AFM, electron microscopy, and small-angle X-ray scattering on immune-isolated porosomes found SNARE proteins VAMP2, syntaxin 1 and SNAP25 in neural porosomes (Naik et al., 2016). During uterine receptivity, particularly on day 5.5, UECs have an increase in the abundance of both t-SNARE (syntaxin 3) and v-SNARE (VAMP2) proteins (Kalam et al., 2020); indicating there is an increase in exocytotic activity trafficked by SNARE proteins during this period. Hence, these SNARE proteins could also be participating in trafficking vesicles to porosomes for partial secretions. The relative activity of the porosome can be seen by the dilation of the porosome base. This dilation is primarily controlled by SNARE proteins (Hou et al., 2014).

5 | CONCLUSION

This study identified for the first time the presence of porosomes as a component of the secretory machinery in UECs during early pregnancy. This investigation also found there was an increase in porosome activity suggesting an increase in partial secretions via porosomes in receptive UECs compared with non-receptive UECs. Thus, this study indicates that "kiss and run" secretion is one of the modes of exocytosis that is active in UECs during early pregnancy and that this form of secretion increases at uterine receptivity.

AUTHOR CONTRIBUTIONS

Sadaf N. Kalam: Conceptualization (lead); data curation (lead); formal analysis (lead); investigation (lead); methodology (lead); project administration (equal); software (lead); writing – original draft (lead); writing – review & editing (lead). **Samson Dowland**: Conceptualization (supporting); formal analysis (supporting); funding acquisition (equal); methodology (supporting); project administration (equal); resources (equal); supervision (equal); writing – review & editing (equal). **Laura Lindsay**: Conceptualization (supporting); funding acquisition (equal); project administration (equal); supervision (equal); writing – review & editing (equal). **Christopher R. Murphy**: Conceptualization (supporting); funding acquisition (lead); investigation (supporting); methodology (supporting); project administration (supporting); resources (lead); supervision (lead); writing – review & editing (equal).

ACKNOWLEDGMENTS

The authors acknowledge the scientific and technical assistance of the Australian Microscopy and Microanalysis Research facility at the Australian Centre for Microscopy & Microanalysis, The University of Sydney. The author also thanks members of the Murphy lab. Financial support was provided by the Australian Research Council, the Ann Macintosh Foundation for the Discipline of Anatomy and Histology and the Murphy Laboratory. Open access publishing facilitated by The University of Sydney, as part of the Wiley - The University of Sydney agreement via the Council of Australian University Librarians.

CONFLICT OF INTEREST

The authors declare no conflict of interest.

DATA AVAILABILITY STATEMENT

The data that support the findings of this study are available on request from the corresponding author. The data are not publicly available due to privacy or ethical restrictions.

ORCID

Sadaf N. Kalam http://orcid.org/0000-0001-8178-6401

REFERENCES

Alberts, B., Johnson, A., Lewis, J., Morgan, D., Raff, M., Roberts, K., & Walter, P. (2008). *Molecular biology of the cell*, 5th edition. Garland Science. https://doi.org/10.1097/01.shk.0000286288.33338.f6

Antonyak, M. A., & Cerione, R. A. (2014). Microvesicles as mediators of intercellular communication in cancer. *Methods in Molecular Biology (Clifton, N.J.)*, *1165*, 147–173. https://doi.org/10.1007/978-1-4939-0856-1_11

Aravanis, A. M., Pyle, J. L., & Tsien, R. W. (2003). Single synaptic vesicles fusing transiently and successively without loss of identity. *Nature*, *423*, 643–647. https://doi.org/10.1038/nature01686

Battey, N. H., James, N. C., Greenland, A. J., & Brownlee, C. (1999). Exocytosis and endocytosis. *The Plant Cell*, *11*(4), 643–659. https://doi.org/10.1105/tpc.11.4.643

Burgess, T. L., & Kelly, R. B. (1987). Constitutive and regulated secretion of proteins. *Annual Review of Cell Biology*, *3*(1), 243–293. https://doi.org/10.1146/annurev.cb.03.110187.001331

Ceccarelli, B., Hurlbut, W. P., & Mauro, A. (1972). Depletion of vesicles from frog neuromuscular junctions by prolonged tetanic stimulation. *Journal of Cell Biology*, *54*(1), 30–38. https://doi.org/10.1083/jcb.54.1.30

Cho, S. J., Wakade, A., Pappas, G. D., & Jena, B. P. (2002). New structure involved in transient membrane fusion and exocytosis. *Annals of the New York Academy of Sciences*, *971*(1), 254–256. https://doi.org/10.1111/j.1749-6632.2002.tb04471.x

Cho, W. J., Jeremic, A., & Jena, B. P. (2005). Direct interaction between SNAP-23 and L-type Ca2+ channel. *Journal of Cellular and Molecular Medicine*, *9*(2), 380–386. https://doi.org/10.1111/j.1582-4934.2005.tb00363.x

Cho, W. J., Jeremic, A., Jin, H., Ren, G., & Jena, B. P. (2007). Neuronal fusion pore assembly requires membrane cholesterol. *Cell Biology*

International, *31*(11), 1301–1308. https://doi.org/10.1016/j.cellbi.2007.06.011

Cho, W. J., Jeremic, A., Rognlien, K. T., Zhvania, M. G., Lazrishvili, I., Tamar, B., & Jena, B. P. (2004). Structure, isolation, composition and reconstitution of the neuronal fusion pore. *Cell Biology International*, *28*(10), 699–708. https://doi.org/10.1016/j.cellbi.2004.07.004

Cho, W. J., Ren, G., Lee, J. S., Jeftinija, K., Jeftinija, S., & Jena, B. P. (2009). Nanoscale 3D contour map of protein assembly within the astrocyte porosome complex. *Cell Biology International*, *33*(2), 224–229. https://doi.org/10.1016/j.cellbi.2008.11.008

Cho, W. J., Shin, L., Ren, G., & Jena, B. P. (2009). Structure of membrane-associated neuronal SNARE complex: Implication in neurotransmitter release. *Journal of Cellular and Molecular Medicine*, *13*(10), 4161–4165. https://doi.org/10.1111/j.1582-4934.2009.00895.x

Craciun, C., & Barbu-Tudoran, L. (2013). Identification of new structural elements within "porosomes" of the exocrine pancreas: A detailed study using high-resolution electron microscopy. *Micron*, *44*(1), 137–142. https://doi.org/10.1016/j.micron.2012.05.011

Drescher, D. G., Cho, W. J., & Drescher, M. J. (2011). Identification of the porosome complex in the hair cell. *Cell Biology International Reports*, *18*(1), 31–34. https://doi.org/10.1042/CBR20110005

Enders, A. C., & Schlafke, S. (1967). A morphological analysis of the early implantation stages in the rat. *American Journal of Anatomy*, *120*(2), 185–225. https://doi.org/10.1002/aja.1001200202

Epand, R. M. (2006). Cholesterol and the interaction of proteins with membrane domains. *Progress in Lipid Research*, *45*(4), 279–294. https://doi.org/10.1016/j.plipres.2006.02.001

Gandolfi, F. (1995). Functions of proteins secreted by oviduct epithelial cells. *Microscopy Research and Technique*, *32*(1), 1–12. https://doi.org/10.1002/jemt.1070320102

Harata, N. C., Aravanis, A. M., & Tsien, R. W. (2006). Kiss-and-run and full-collapse fusion as modes of exo-endocytosis in neurosecretion. *Journal of Neurochemistry*, *97*(6), 1546–1570. https://doi.org/10.1111/j.1471-4159.2006.03987.x

Holt, O. J., Gallo, F., & Griffiths, G. M. (2006). Regulating secretory lysosomes. *Journal of Biochemistry*, *140*(1), 7–12. https://doi.org/10.1093/jb/mvj126

Hoshino, Y., Shannon, Jr., A. W., & Seligman, A. M. (1976). A study on ferrocyanide-reduced osmium tetroxide as a stain and cytochemical agent. *Acta Histochemica et Cytochemica*, *9*(2), 125–136. https://doi.org/10.1267/ahc.9.125

Hou, X., Lewis, K. T., Wu, Q., Wang, S., Chen, X., Flack, A., Mao, G., Taatjes, D. J., Sun, F., & Jena, B. P. (2014). Proteome of the porosome complex in human airway epithelia: Interaction with the cystic fibrosis transmembrane conductance regulator (CFTR). *Journal of Proteomics*, *96*, 82–91. https://doi.org/10.1016/j.jprot.2013.10.041

Jamieson, J. D., & Palade, G. E. (1967a). Intracellular transport of secretory proteins in the pancreatic exocrine cell. I. Role of the peripheral elements of the Golgi complex. *The Journal of Cell Biology*, *34*(2), 577–596. https://doi.org/10.1083/jcb.34.2.577

Jamieson, J. D., & Palade, G. E. (1967b). Intracellular transport of secretory proteins in the pancreatic exocrine cell. II. Transport to condensing vacuoles and zymogen granules. *The Journal of Cell Biology*, *34*(2), 597–615. https://doi.org/10.1083/jcb.34.2.597

Jena, B. P. (2004). Discovery of the porosome: Revealing the molecular mechanism of secretion and membrane fusion in cells. *Journal of Cellular and Molecular Medicine*, *8*(1), 1–21. https://doi.org/10.1111/j.1582-4934.2004.tb00255.x

Jena, B. P. (2009). Functional organization of the porosome complex and associated structures facilitating cellular secretion. *Physiology*, *24*(6), 367–376. https://doi.org/10.1152/PHYSIOL.00021.2009

Jeremic, A., Cho, W. J., & Jena, B. P. (2004). Membrane fusion: What may transpire at the atomic level. *Journal of Biological Physics and Chemistry*, *4*, 139–142. https://pdfs.semanticscholar.org/043d/97ddcd67344a5c2cc203922f187f86d689ea.pdf

Jeremic, A., Cho, W. J., & Jena, B. P. (2006). Cholesterol is critical to the integrity of neuronal porosome/fusion pore. *Ultramicroscopy*, *106*(8–9), 674–677. https://doi.org/10.1016/j.ultramic.2006.01.012

Jeremic, A., Kelly, M., Cho, J. A., Cho, S. -J., Horber, J. K. H., & Jena, B. P. (2004). Calcium drives fusion of SNARE-apposed bilayers. *Cell Biology International*, *28*(1), 19–31. https://doi.org/10.1016/j.cellbi.2003.11.004

Jeremic, A., Kelly, M., Cho, S. J., Stromer, M. H., & Jena, B. P. (2003). Reconstituted fusion pore. *Biophysical Journal*, *85*(3), 2035–2043. https://doi.org/10.1016/S0006-3495(03)74631-1

Kalam, S. N., Cole, L., Lindsay, L., & Murphy, C. R. (2020). Membrane trafficking directed by VAMP2 and syntaxin 3 in uterine epithelial cells. *Reproduction*, *160*(4), 533–546. https://doi.org/10.1530/REP-20-0233

De Los Santos, M. J., Apter, S., Coticchio, G., Debrock, S., Lundin, K., Plancha, C. E., Prados, F., Rienzi, L., Verheyen, G., Woodward, B., & Vermeulen, N. (2016). Revised guidelines for good practice in IVF laboratories (2015) The ESHRE Guideline Group on Good Practice in IVF Labs. *Human Reproduction (Oxford, England)*, *31*(4), 685–686. https://doi.org/10.1093/humrep/dew016

Kalam, S. N., Dowland, S., Lindsay, L., & Murphy, C. R. (2018). Microtubules are reorganised and fragmented for uterine receptivity. *Cell and Tissue Research*, *374*, 667–677. https://doi.org/10.1007/s00441-018-2887-x

Karnovsky, M. J. (1971). Use of ferrocyanide-reduced osmium tetroxide in electron microscopy. *American Society for Cell Biology*, *146*(1971): A284.

Lee, J. S., Cho, W. J., Jeftinija, K., Jeftinija, S., & Jena, B. P. (2009). Porosome in astrocytes. *Journal of Cellular and Molecular Medicine*, *13*(2), 365–372. https://doi.org/10.1111/j.1582-4934.2008.00334.x

Lindsay, L. A., & Murphy, C. R. (2006). Redistribution of aquaporins 1 and 5 in the rat uterus is dependent on progesterone: A study with light and electron microscopy. *Reproduction*, *131*(2), 369–378. https://doi.org/10.1530/rep.1.00914

McManaman, J. L., Reyland, M. E., & Thrower, E. C. (2006). Secretion and fluid transport mechanisms in the mammary gland: Comparisons with the exocrine pancreas and the salivary gland. *Journal of Mammary Gland Biology and Neoplasia*, *11*(3–4), 249–268. https://doi.org/10.1007/s10911-006-9031-3

Mohrmann, R., de Wit, H., Verhage, M., Neher, E., & Sorensen, J. B. (2010). Fast vesicle fusion in living cells requires at least three SNARE complexes. *Science*, *330*(6003), 502–505. https://doi.org/10.1126/science.1193134

Murphy, C. R. (1993). The plasma membrane of uterine epithelial cells: Structure and histochemistry. *Progress in Histochemistry and Cytochemistry*, *27*(3), 1–66. https://doi.org/10.1016/S0079-6336(11)80004-5

Murphy, C. R. (1994). Plasma membrane transformation: A common response of uterine epithelial cells during the peri-implantation period. *Cell Biology International*, *18*(12), 1115–1128. https://doi.org/10.1006/cbir.1994.1038

Murphy, C. R. (2001). The plasma membrane transformation: A key concept in uterine receptivity. *Reproductive Medicine Review*, *9*(03), 197–208. https://doi.org/10.1017/S0962279901000321

Murphy, C. R. (2004). Uterine receptivity and the plasma membrane transformation. *Cell Research*, *14*(4), 259–267. https://doi.org/10.1038/sj.cr.7290227

Murphy, C. R., & Dwarte, D. M. (1987). Increase in cholesterol in the apical plasma membrane of uterine epithelial cells during early pregnancy in the rat. *Acta Anat (Basel)*, *128*(1), 76–79. http://www.ncbi.nlm.nih.gov/entrez/query.fcgi?cmd=Retrieve%26db=PubMed%26dopt=Citation%26list_uids=3825491

Murphy, C. R., & Martin, B. (1985). Cholesterol in the plasma membrane of uterine epithelial cells: A freeze-fracture cytochemical study with digitonin. *Journal of Cell Science*, *78*, 163–172. http://www.ncbi.nlm.nih.gov/pubmed/4093470%5Cnhttp://jcs.biologists.org/content/78/1/163.full.pdf

Murphy, C. R., & Martin, B. (1987). Digitonin cytochemistry reveals cholesterol-rich vesicles in uterine epithelial cells. *Acta Histochemica*, *81*(2), 143–147. https://doi.org/10.1016/S0065-1281(87)80003-X

Naik, A. R., Kulkarni, S. P., Lewis, K. T., Taatjes, D. J., & Jena, B. P. (2015). Functional reconstitution of the insulin-secreting *porosome* complex in live cells. *Endocrinology*, *157*(1), 54–60. https://doi.org/10.1210/en.2015-1653

Naik, A. R., Lewis, K. T., & Jena, B. P. (2016). The neuronal porosome complex in health and disease. *Experimental Biology and Medicine*, *241*(2), 115–130. https://doi.org/10.1177/1535370215598400

Nieder, G. L., & Macon, G. R. (1987). Uterine and oviducal protein secretion during early pregnancy in the mouse. *Journal of Reproduction and Fertility*, *81*(1), 287–294. http://www.ncbi.nlm.nih.gov/pubmed/3668958

O'Neil, E. V., Burns, G. W., & Spencer, T. E. (2020). Extracellular vesicles: Novel regulators of conceptus-uterine interactions. *Theriogenology*, *150*, 106–112. https://doi.org/10.1016/J.THERIOGENOLOGY.2020.01.083

Parr, M. M. (1982). Apical vesicles in the rat uterine epithelium during early pregnancy: A morphometric study, *Biology of Reproduction*, *26*(5), 915–924. http://eutils.ncbi.nlm.nih.gov/entrez/eutils/elink.fcgi?dbfrom=pubmed%26id=7201330%26retmode=ref%26cmd=prlinks%5Cnpapers2://publication/doi/10.1095/biolreprod26.5.915.

Pickett, J. A., & Edwardson, J. M. (2006). Compound exocytosis: Mechanisms and functional significance. *Traffic*, *7*(2), 109–116. https://doi.org/10.1111/j.1600-0854.2005.00372.x

Poste, G., & Allison, A. C. (1973). Membrane fusion. *Biochimica et Biophysica Acta*, *300*(4), 421–465. http://www.ncbi.nlm.nih.gov/pubmed/4360422

Preston, A. M., Lindsay, L. A., & Murphy, C. R. (2006). Desmosomes in uterine epithelial cells decrease at the time of implantation: An ultrastructural and morphometric study. *Journal of Morphology*, *267*(1), 103–108. https://doi.org/10.1002/jmor.10390

Schneider, S. W., Sritharan, K. C., Geibel, J. P., Oberleithner, H., & Jena, B. P. (1997). Surface dynamics in living acinar cells imaged by atomic force microscopy: Identification of plasma membrane structures involved in exocytosis. *Proceedings of the National Academy of Sciences of the United States of America*, *94*(1), 316–321. http://www.ncbi.nlm.nih.gov/pubmed/8990206

Schramm, M. (1967). Secretion of enzymes and other macromolecules. *Annual Review of Biochemistry*, *36*(1), 307–320. https://doi.org/10.1146/annurev.bi.36.070167.001515

Söllner, T., Whiteheart, S. W., Brunner, M., Erdjument-Bromage, H., Geromanos, S., Tempst, P., & Rothman, J. E. (1993). SNAP receptors implicated in vesicle targeting and fusion. *Nature*, *362*(6418), 318–324. https://doi.org/10.1038/362318a0

Strandell, A., & Lindhard, A. (2002). Why does hydrosalpinx reduce fertility?: The importance of hydrosalpinx fluid. *Human Reproduction*, *17*(5), 1141–1145. https://doi.org/10.1093/humrep/17.5.1141

Sutton, R. B., Fasshauer, D., Jahn, R., & Brunger, A. T. (1998). Crystal structure of a SNARE complex involved in synaptic exocytosis at 2.4 A resolution. *Nature*, *395*(6700), 347–353. https://doi.org/10.1038/26412

Tachi, S., Tachi, C., & Lindner, H. R. (1970). Ultrastructural features of blastocyst attachment and trophoblastic invasion in the rat. *Reproduction*, *21*(1), 37–56. https://doi.org/10.1530/jrf.0.0210037

Taguchi, T. (2013). Emerging roles of recycling endosomes. *Journal of Biochemistry*, *153*(6), 505–510. https://doi.org/10.1093/jb/mvt034

Taraska, J. W., Perrais, D., Ohara-Imaizumi, M., Nagamatsu, S., & Almers, W. (2002). Secretory granules are recaptured largely intact after stimulated exocytosis in cultured endocrine cells. *PNAS*, *100*(4), 2070–2075. https://doi.org/10.1073/pnas.0337526100

Tkach, M., & Thé Ry, C. (2016). Leading edge review communication by extracellular vesicles: Where we are and where we need to go. *Cell*, *164*, 1226–1232. https://doi.org/10.1016/j.cell.2016.01.043

Tojima, T., Yamane, Y., Takagi, H., Takeshita, T., Sugiyama, T., Haga, H., Kawabata, K., Ushiki, T., Abe, K., Yoshioka, T., & Ito, E. (2000). Three-dimensional characterization of interior structures of exocytotic apertures of nerve cells using atomic force microscopy. *Neuroscience*, *101*(2), 471–481. https://doi.org/10.1016/S0306-4522(00)00320-1

Tuma, P. L., & Hubbard, A. L. (2003). Transcytosis: Crossing cellular barriers. *Physiological Reviews*, *83*(3), 871–932. https://doi.org/10.1152/physrev.00001.2003

How to cite this article: Kalam, S. N., Dowland, S., Lindsay, L., & Murphy, C. R. (2022). Porosomes in uterine epithelial cells: Ultrastructural identification and characterisation during early pregnancy. *Journal of Morphology*, 283, 1381–1389. https://doi.org/10.1002/jmor.21504